Contribution No. 7673 from the Arthur Amos Noyes Laboratory, California Institute of Technology, Pasadena, California 91125

Electronic Absorption Spectra of Binuclear Rhodium(I) Isocyanide Complexes. Comparison of Ground-State and $d\sigma^* \rightarrow p\sigma$ Excited-State Bond Energies

Steven F. Rice, Vincent M. Miskowski, and Harry B. Gray*

Received October 2, 1987

The polarized single-crystal absorption spectra of $[Rh_2b_4](BPh_4)_2 \cdot CH_3CN$ and $[Rh_2(TMB)_4](BPh_4)_2$ have been measured and analyzed (b = 1,3-diisocyanopropane; TMB = 2,5-diisocyano-2,5-dimethylhexane). The results indicate that the fully allowed transitions near 550 and 310 nm in these d^8-d^8 complexes are $^1A_1 \rightarrow {}^1A_2$ ($d\sigma^* \rightarrow p\sigma$) and $^1A_1 \rightarrow {}^1E$ (d_{xz}, $d_{yz} \rightarrow p\sigma$), respectively ($D_4$ point group designations). The weak singlet → triplet systems associated with both excitations also have been identified. The vibronic structure of the $^1A_{1g} \rightarrow {}^3A_{2u}$ system of $Rh_2b_4^{2+}$ has been analyzed in detail. The Rh-Rh bond length in the $^3A_{2u}$ state of $Rh_2b_4^{2+}$ is estimated from a Franck-Condon analysis to be 2.93 Å (the ground-state value is 3.24 Å). The ground-state and excited-state Rh-Rh bond energies are estimated to be 12 ± 6 and 36 ± 6 kcal/mol, respectively.

Square-planar d^8 complexes[1] can assemble into extended one-dimensional systems that exhibit unusual properties.[2] We have been investigating dimers of d^8 complexes[3-5] in an effort to understand the properties of more extended systems.

We have performed detailed spectroscopic studies of binuclear rhodium(I) complexes bridged by four diisocyanide ligands, where the ligand is either b (1,3-diisocyanopropane) or TMB (2,5-diisocyano-2,5-dimethylhexane). A preliminary report has been published.[6] Our aim is to assess the relative importance of the two types[3,4] of potentially strong σ metal-metal bonding interactions available to these complexes, one between $4d_{z^2}$ orbitals, yielding $d\sigma$ and $d\sigma^*$ (filled in the ground state), and the other between $5p_z$ orbitals, producing $p\sigma$ and $p\sigma^*$ (empty in the ground state).

Experimental Section

The diisocyanide ligands b and TMB were prepared by literature procedures,[4] as were the compounds $[Rh_2b_4](BPh_4)_2$ and $[Rh_2(TMB)_4](PF_6)_2$.

Large platelike single crystals of $[Rh_2b_4](BPh_4)_2 \cdot CH_3CN$ were grown by overnight cooling of a hot saturated CH_3CN solution. The well-developed crystal face of the monoclinic[4b] crystals was determined to be (100) by X-ray photographic methods, and the orientation of the crystallographic *b* axis was determined to be parallel with the strongly absorbing extinction of the highly dichroic crystals.

The compound $[Rh_2(TMB)_4](BPh_4)_2$ was prepared by addition of a methanol solution of $Na(BPh_4)$ to a concentrated solution of $[Rh_2(TMB)_4](PF_6)_2$ in methanol. A red precipitate was obtained. A 10-mg sample of this material was dissolved in 20 mL of CH_3CN, and water was added to the cloud point; a small amount of CH_3CN was added to give a clear solution, which was allowed to evaporate over several days. Large but extremely thin (2 mm × 2 mm × <30 μm) single crystals formed on the surface of the solution (it is likely that these crystals contain some CH_3CN). Because of the unusual morphology of the crystals, attempts to characterize them by X-ray crystallographic methods were unsuccessful. However, the well-developed crystal face was very strongly dichroic and displayed wavelength-independent extinctions.

Salts of $Rh(CNPh)_4^+$ and $Rh(CNCMe_3)_4^+$ were prepared by literature procedures.[3c] Electronic absorption spectra were obtained as described previously.[5] Poly(methyl methacrylate) (PMMA) films incorporating the various Rh^I compounds were obtained by slow evaporation of CH_2Cl_2 solutions.

Results and Discussion

Electronic Spectra. Figure 1 shows the low-temperature spectrum of $[Rh_2b_4](BPh_4)_2$ in a PMMA film, which is typical of our low-temperature isotropic data. Previous studies[4a,b] have assigned the strong bands at 565 and 319 nm to respectively the fully allowed $^1A_{1g} \rightarrow {}^1A_{2u}$ ($d\sigma^* \rightarrow p\sigma$) and $^1A_{1g} \rightarrow {}^1E_u$ (d_{xz}, $d_{yz} \rightarrow p\sigma$) excitations.[7] It is noteworthy that the lower energy maximum red-shifts from the room-temperature value of 555 nm as the temperature is decreased (the band simultaneously narrows and increases in peak intensity). According to band-moment theory,[8] the red shift of the maximum indicates that the effective vibrational frequency that is coupled to the electronic transition is higher in the excited state than in the ground state.

Two weaker bands are observed to either side of the $^1A_{1g} \rightarrow {}^1E_u$ transition. The band at 342 nm is assigned to a spin-forbidden transition, $^1A_{1g} \rightarrow {}^3E_u$, while that at ~298 nm is attributable to one quantum of the $\nu(C{\equiv}N)$ stretch (~2150 cm^{-1}) built on the electronic origin, which is consistent with the presence of MLCT character[1] in the d → p excited state. Additional structured absorption below 280 nm is due to the BPh_4^- anions.

Figure 2 shows polarized single-crystal spectra for $[Rh_2(TMB)_4](BPh_4)_2$. We do not know the crystal structure of this salt,[9] but the very large and opposite polarization ratios for the two intense bands imply that the Rh-Rh axis must lie nearly exactly in the plane of the crystal face.

Since we know that the 533-nm band is *z*-polarized (vide infra), the bands at 316 and 342 nm must both be *x*,*y*-polarized (molecular axes). This is consistent with the assignments already given, provided that the 342-nm feature is the E component of ^3E. The D_4 double group representation of ^3E yields states of E, A_1, A_2, B_1, and B_2 symmetries. Of these, the A_2 component also yields a dipole-allowed electronic transition from the ground state, but with molecular *z* polarization. This is our assignment for the 335-nm feature in the ∥ spectrum. The relative energies of the two ^3E components are very reasonable; spin-orbit coupling of

(1) (a) Gray, H. B.; Ballhausen, C. J. *J. Am. Chem. Soc.* **1963**, *85*, 260-265. (b) Cowan, C. D.; Gray, H. B. *Inorg. Chem.* **1976**, *15*, 2823-2824.

(2) (a) Interrante, L. In *Extended Interactions Between Metal Ions in Transition Metal Complexes*; Interrante, L., Ed.; American Chemical Society: Washington, DC, 1974. (b) Miller, J. S.; Epstein, A. J. *Prog. Inorg. Chem.* **1976**, *20*, 1-151.

(3) (a) Mann, K. R.; Gray, H. B. *Adv. Chem. Ser.* **1979**, No. *173*, 225-235. (b) Mann, K. R.; Gordon, J. G., II; Gray, H. B. *J. Am. Chem. Soc.* **1975**, *97*, 3553-3555. (c) Mann, K. R.; Lewis, N. S.; Williams, R. M.; Gray, H. B.; Gordon, J. G., II *Inorg. Chem.* **1978**, *17*, 828-834.

(4) (a) Miskowski, V. M.; Nobinger, G. L.; Kliger, D. S.; Hammond, G. S.; Lewis, N. S.; Mann, K. R.; Gray, H. B. *J. Am. Chem. Soc.* **1978**, *100*, 485-488. (b) Mann, K. R.; Thich, J. A.; Bell, R. A.; Coyle, C. L.; Gray, H. B. *Inorg. Chem.* **1980**, *19*, 2462-2468. (c) Rice, S. F.; Milder, S. J.; Gray, H. B.; Goldbeck, R. A.; Kliger, D. S. *Coord. Chem. Rev.* **1982**, *43*, 349-354.

(5) (a) Rice, S. F.; Gray, H. B. *J. Am. Chem. Soc.* **1983**, *105*, 4571-4575. (b) Stiegman, A. E.; Rice, S. F.; Gray, H. B.; Miskowski, V. M. *Inorg. Chem.* **1987**, *26*, 1112-1116.

(6) Rice, S. F.; Gray, H. B. *J. Am. Chem. Soc.* **1981**, *103*, 1593-1595.

(7) The symmetry designations for $Rh_2b_4^{2+}$ are those for the D_{4h} point group, as the crystal structure[4b] indicates eclipsed isocyanide groups. More generally, we will drop the g, u subscripts, according to the D_4 symmetry afforded by the torsionally rotated structure[4b] of $Rh_2(TMB)_4^{2+}$.

(8) Ballhausen, C. J. *Molecular Electronic Structures of Transition Metal Complexes*; McGraw-Hill: New York, 1979; pp 132-135.

(9) However, the structure of $[Ir_2(TMB)_4](BPh_4)_2 \cdot 2CH_3CN$, crystallized from CH_3CN, has been determined (Smith, D. C.; Schaefer, W. P., unpublished work). This monoclinic ($P2_1/n$) structure places the Ir-Ir vectors at solid angles of only 4° from the *b* axis. A similar structure for the Rh^I complex would be consistent with our polarized single-crystal spectra.

0020-1669/88/1327-4704$01.50/0

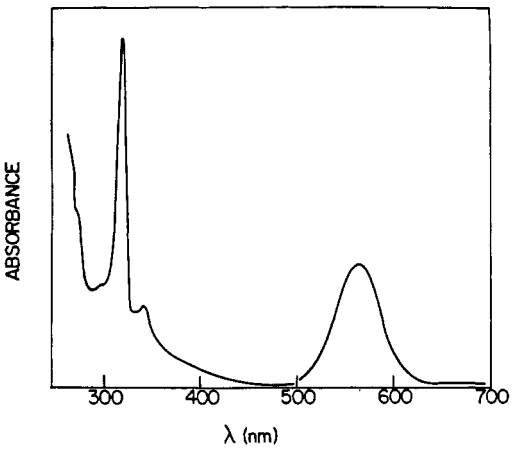

Figure 1. Electronic absorption spectrum of $[Rh_2b_4](BPh_4)_2$ in a PMMA film at 15 K.

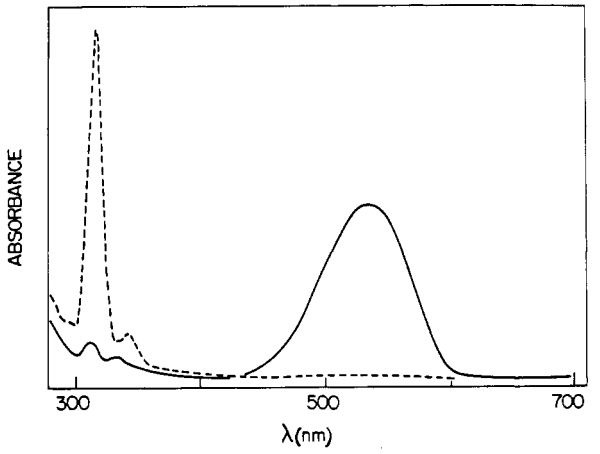

Figure 2. Single-crystal absorption spectra of a very thin (~0.3 μm) crystal of $[Rh_2(TMB)_4](BPh_4)_2$ at 300 K: parallel polarization (—); perpendicular polarization (---).

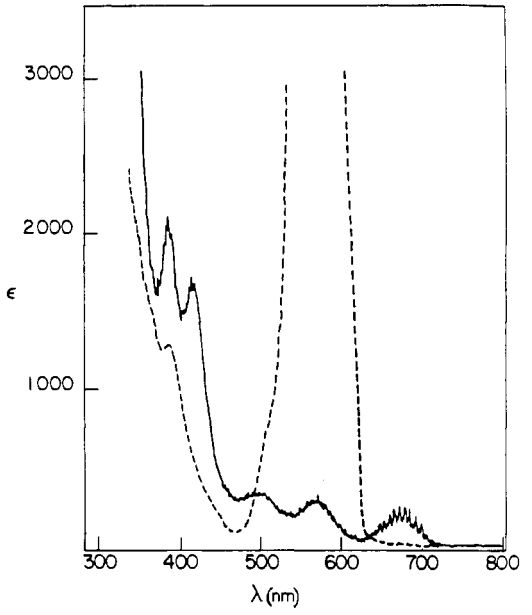

Figure 3. Single-crystal absorption spectra of a thin crystal of $[Rh_2b_4](BPh_4)_2{\cdot}CH_3CN$ at 5 K: $\|b$ polarization (---); $\perp b$ polarization (—).

E(^{1}E) and E(^{3}E) should push the latter to lower energy, while coupling of $A_2(^3E)$ with the 533-nm $A_2(^1A_2)$ should have the opposite effect. An additional weak feature in the $\|$ spectrum is nearly coincident with the $\perp$-polarized ^{1}E transition and likely represents vibronically induced "off"-polarization intensity of this transition and/or a slight crystallographic misalignment of the rhodium–rhodium vector with the crystal face.

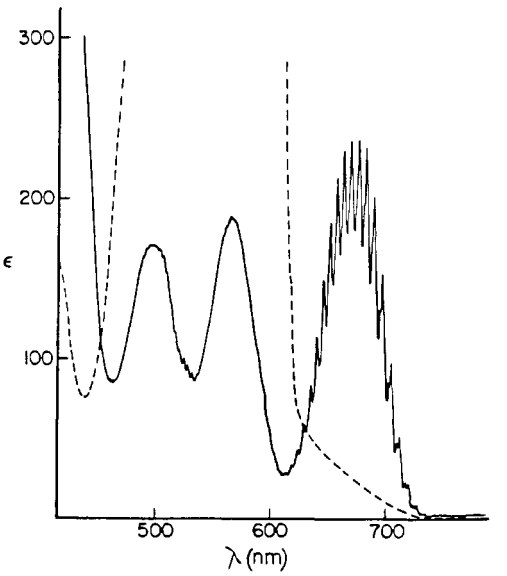

Figure 4. Spectra of a crystal thicker than the one employed for Figure 3.

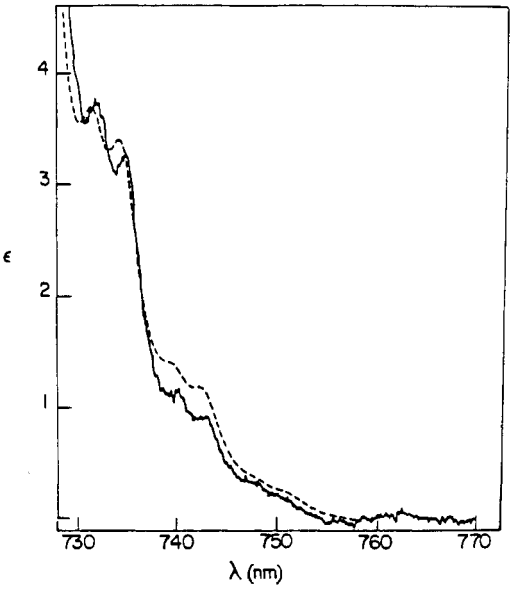

Figure 5. Spectrum of a crystal thicker than the one employed for Figure 4. The dashed line is a calculated spectrum (see text); E_0 = 13 310 cm^{-1} (751.5 nm).

The single-crystal low-temperature spectra of $[Rh_2b_4](BPh_4)_2{\cdot}CH_3CN$ for a range of crystal thicknesses are shown in Figures 3–5. The rhodium–rhodium vector lies rigorously in the crystal face that was studied, and spectra were recorded for the extinctions $\|$ ($\|b$) and $\perp$ ($\perp b$) to molecular z.

The ~565-nm band is confirmed to be polarized $\|z$, consistent with the $^1A_{1g} \rightarrow {}^1A_{2u}$ ($d\sigma^* \rightarrow p\sigma$) assignment given above. A number of weaker features are also resolved. One of these in $\perp z$ polarization, at 568 nm, is nearly coincident with the allowed $\|z$ band and is assigned to vibronically induced $\perp z$ intensity of the $^1A_{1g} \rightarrow {}^1A_{2u}$ transition, presumably involving modes of e_g symmetry. The fact that the intensity of this feature decreases by a factor of 2 as the temperature is reduced from room temperature to 5 K is consistent with the vibronic interpretation.

We interpret features in $\|z$ polarization at ~505 nm (sh) and in $\perp z$ polarization at ~500 nm as being due to one quantum of ν(C≡N) (a_{1g} and e_g modes in the $\|$ and $\perp$ polarizations) built on the $^1A_{1g} \rightarrow {}^1A_{2u}$ transition. As was the case for ^1E_u, a very small amount of π^*(C≡N) character apparently is present in the $^1A_{2u}$ state.

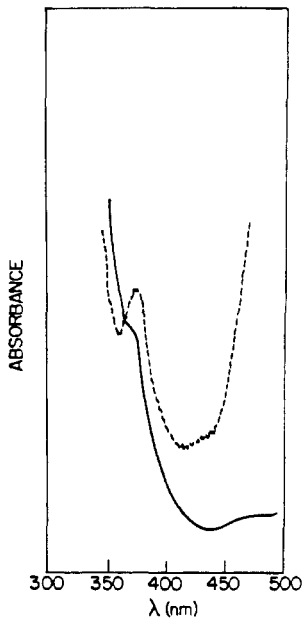

Figure 6. Absorption spectra of $[Rh_2(TMB)_4](BPh_4)_2$ at 5 K: parallel polarization (- - -); perpendicular polarization (—).

The highly vibronically structured feature maximizing at ~670 nm is attributable to the $^1A_{1g} \rightarrow E_u$ ($^3A_{2u}$) $d\sigma^* \rightarrow p\sigma$ transition. The $^3A_{2u}$ state also yields an A_{1u} spin–orbit component, to which transitions from the ground state would be highly forbidden.[10] The vibronic structure of this band consists of a very long progression[6] in a frequency of 143 cm^{-1}. Resonance Raman studies[11] of the ground and excited states indicate that this frequency is the excited-state stretch, $\nu(Rh_2)$, which is greatly increased from the ground-state value (85 cm^{-1}).[12] This is consistent with simple molecular orbital arguments,[4a] which predict a stronger metal–metal bond in the $d\sigma^* \rightarrow p\sigma$ excited state. The lower energy vibronic features also show sidebands separated from the pure $\nu(Rh_2)$ progression by 60 cm^{-1}. The probable assignment of the sidebands is to a ligand deformation mode.

Low-temperature luminescence of $[Rh_2b_4](BPh_4)_2{\cdot}CH_3CN$ (fluorescence and phosphorescence)[4] showed little vibronic structure, which is disappointing, but reasonable in terms of the low ground-state $\nu(Rh_2)$.

Several additional weak absorptions are observed. First, we see a reproducible but very weak vibronic progression centered at ~520 nm in $\perp z$ polarization, in the valley between the two broad features that maximize at 500 and 568 nm (Figure 4). The frequency differences between the vibronic lines are all ~130 cm^{-1}. We do not think that these lines are associated with the stronger features because the frequency interval is significantly less than that of $^1A_{1g} \rightarrow {}^3A_{2u}$. While we have not been able to directly measure $\nu(Rh_2)$ for the $^1A_{2u}$ excited state, studies of $Pt_2(P_2O_5H_2)_4^{4-}$ have shown that the $\nu(Pt_2)$ values for the $^1A_{2u}$ and $^3A_{2u}$ ($d\sigma^* \rightarrow p\sigma$) excited states are virtually identical.[5b]

The very low intensity signals a highly forbidden transition, while the $\nu(Rh_2)$ of 130 cm^{-1} indicates a slightly less strongly metal–metal-bonded state than $^3A_{2u}$ ($d\sigma^* \rightarrow p\sigma$). Axial $d \rightarrow p$ transitions that might fit this description are $d\sigma \rightarrow p\sigma$ and $d\sigma^* \rightarrow p\sigma^*$. Both are $A_{1g} \rightarrow A_{1g}$ transitions, hence dipole-forbidden. According to the arguments set out in the next section, it seems unlikely that $d\sigma \rightarrow p\sigma$ excited states could have as strong a metal–metal bond as is experimentally indicated, so we favor a $d\sigma^* \rightarrow p\sigma^*$ assignment. However, it should be noted that these two excitations can mix with each other. The extreme weakness of the transition suggests assignment to the spin-forbidden $^1A_{1g} \rightarrow {}^3A_{1g}$ excitation.

Finally, we see weak bands for $Rh_2b_4^{2+}$ at 385 and 415 nm (Figure 3). The latter has $\perp z$ polarization, while the former has mixed polarization. A thick crystal of $[Rh_2(TMB)_4](BPh_4)_2$ also shows a band in this spectral region (at 380 nm, with mixed polarization: Figure 6).

We have considered many possible assignments for these features. One initially attractive assignment was to excitations into the $d\sigma^*$(Rh–C) orbitals derived from $Rh^I d_{x^2-y^2}$, as excited states of this type have been postulated[4c] to be thermally accessible from $^3A_{2u}$ ($d\sigma^* \rightarrow p\sigma$). However, bands associated with transitions to these excited states are expected to be very broad, because of large excited-state distortions along the metal–ligand stretching coordinate, whereas the observed weak bands are narrow, with widths comparable to those of the assigned $d \rightarrow p_z$ absorptions. Most importantly, the third-transition-series analogue $Ir_2(TMB)_4^{2+}$ shows[13] a similarly weak absorption band at 420 nm. As d–d electronic transitions to $d\sigma^*$(M–L) levels are known[14] to strongly blue-shift in 5d complexes, the d–d hypothesis must be abandoned.

There are several remaining possible assignments involving $d \rightarrow p_z$ transitions. A very attractive one would invoke the $d_{xy} \rightarrow p_z$ derived transitions ($d\delta, \delta^* \rightarrow p\sigma$), which are dipole-forbidden for both mononuclear[1] and binuclear d^8 complexes, and one of these excitations is a likely possibility for the ~380-nm band of the rhodium complexes. A problem with this assignment for the 415-nm $\perp z$ polarized band of $[Rh_2b_4](BPh_4)_2{\cdot}CH_3CN$ is that it has no analogue in the $[Rh_2(TMB)_4](BPh_4)_2$ spectrum. While differences in site symmetry could account for this apparent discrepancy, another possible assignment for the 415-nm band is suggested by our tentative placement of $^1A_{1g} \rightarrow {}^3A_{1g}$ ($d\sigma^* \rightarrow p\sigma^*$) at 520 nm. The 415-nm band could then be $^1A_{1g} \rightarrow {}^1A_{1g}$ ($d\sigma^* \rightarrow p\sigma^*$),[15] and the blue shift seen for the lower energy $d\sigma^* \rightarrow p\sigma$ transitions (TMB vs b), if it also occurs for $d\sigma^* \rightarrow p\sigma^*$, could account for the difficulty in locating the band in the TMB complex.

Relative Importance of d–d and p–p Metal–Metal Bonding. The weak ground-state metal–metal bond in d^8–d^8 complexes has been attributed to mixing of the filled $d\sigma/d\sigma^*$ set with the empty $p\sigma/p\sigma^*$ orbitals, as a formal metal–metal bond order of 0 would otherwise result. The metal–metal bond lengths in the d^8–d^8 dimers (~3.25 Å for Rh–Rh)[3,4] seem to be too long for good $4d_{z^2}$–$4d_{z^2}$ overlap between the metal centers, but the $4d_{z^2}$–$5p_z$ overlap could be large.

A problem with this interpretation is that binuclear transitions derived from $d_{xz}, d_{yz} \rightarrow p_z$ electronic transitions, e.g., $^1A_{1g} \rightarrow {}^1E_u$, consistently have energies and widths that are nearly identical with those of mononuclear analogues.[4,5] It is very difficult to ascribe much metal–metal bonding to the $p\sigma$ orbital, given these experimental observations.

We have suggested elsewhere[5b] that the ground-state metal–metal distances may already be optimized for 5p–5p/5p–4d metal–metal bonding, which would account for the narrow widths of the $d_{xz}, d_{yz} \rightarrow p_z$ excitations; metal–metal bond lengths would be unaffected in these dimer excited states. However, the energetic insensitivity of the transitions to dimerization suggests, in addition, that the metal–metal p–p interaction is intrinsically weak. This does not preclude it from accounting for the weak ground-state bonding (vide infra). Indeed, most of the attractive p–p/p–d interaction may already be included in the ground state by configuration mixing.

The $d_{z^2} \rightarrow p_z$ excitations, on the other hand, are very strongly affected by dimerization, with the maximum of the lowest such singlet–singlet excitation shifting from 386 nm in $Rh(CNCMe_3)_4^+$

(10) Studies of d^8–d^8 $Pt_2(P_2O_5H_2)_4^{4-}$ have indicated that the A_{1u} spin–orbit state lies just below the E_u spin–orbit state; see ref 5 and references therein.

(11) Dallinger, R. F.; Miskowski, V. M.; Gray, H. B.; Woodruff, W. H. *J. Am. Chem. Soc.* **1981**, *103*, 1595–1596.

(12) We observed a progression of the $\nu(Rh_2)$ fundamental plus two overtones for the 85-cm^{-1} line of the $[Rh_2b_4](BPh_4)_2{\cdot}CH_3CN$ crystal (514.5-nm Ar^+ laser excitation). The $\nu(Rh_2)$ value has been reported to be 79 cm^{-1} in CH_3CN solution.[11]

(13) Smith, D. C.; Miskowski, V. M., unpublished results.

(14) Miskowski, V. M.; Gray, H. B. *Comments Inorg. Chem.* **1985**, *4*, 323–327.

(15) The observed $\perp z$ polarization is consistent with the crystallographic $m(z)$ site symmetry,[4b] as an $A_{1g} \rightarrow A_{1g}$ transition transforms as $A'(x,y)$ in the C_s point group.

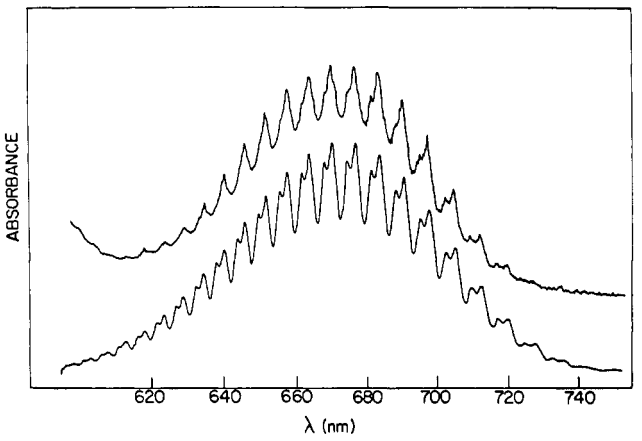

Figure 7. $^1A_{1g} \rightarrow {}^3A_{2u}$ absorption band of $[Rh_2b_4](BPh_4)_2 \cdot CH_3CN$ (upper); calculated band (lower).

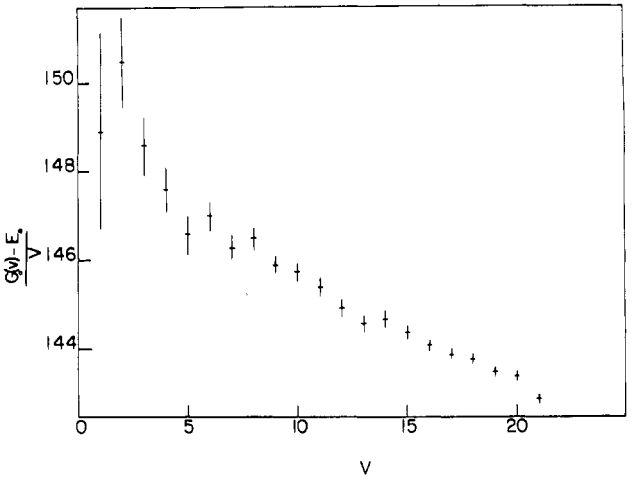

Figure 8. Birge–Sponer plot $[(G_0(v) - E_0)/v$ vs $v]$ of the $^3A_{2u}$ vibronic energy levels in $[Rh_2b_4](BPh_4)_2 \cdot CH_3CN$.

to 553 nm in $Rh_2b_4^{2+}$ (CH_3CN solution, 25 °C). It seems reasonable to attribute this shift to the d_{z^2}–d_{z^2} interaction of the two metal centers, with the excited state showing a much stronger metal–metal bond (bond order $\sim{}^1/_2$) because of depopulation of the $d\sigma^*$ orbital.

Excited-State Distortions. Because of the detailed vibronic structure resolved for the $^1A_{1g} \rightarrow E_u$ ($^3A_{2u}$) $d\sigma^* \rightarrow p\sigma$ transition of $[Rh_2b_4](BPh_4)_2 \cdot CH_3CN$, it is possible to get a good estimate of the excited-state distortion along the rhodium–rhodium normal coordinate. We attacked the problem by simulating the observed band by Franck–Condon calculations. The results[16] are compared to the observed band in Figure 7, while the origin regions are compared in Figure 5. Ground- and excited-state frequencies assumed were 85 and 149 cm^{-1}, respectively, a Lorentzian line width of 70 cm^{-1} was taken from the experimental spectra, and the only parameter varied was the distortion $|\Delta Q|$, the derived value of which is 0.31 Å if the effective mass of the oscillator is assumed to be the reduced mass of Rh_2. From the ground-state bond distance of 3.24 Å and on the assumption that ΔQ is negative, on the basis of the frequency increase in the excited state, the excited-state bond distance is therefore 2.93 Å. This distance is in excellent agreement with the 2.94 Å obtained from Woodruff's correlation[17] for a frequency of 149 cm^{-1} (Rh_2 force constant 0.673 mdyn/Å).

The two-electron-oxidized complex, $Rh_2b_4Cl_2^{2+}$, with a d^7–d^7 single metal–metal bond, has a Rh–Rh distance of 2.83 Å and a $\nu(Rh_2)$ of 134 cm^{-1}.[18] The latter needs to be corrected[18] for axial ligand effects (mass, and mixing with $\nu(RhCl)$), and the resulting "diatomic" $\nu(Rh_2)$ and force constant are $\sim$180 cm^{-1} and $\sim$1 mdyn/Å.

The ground-state $\nu(Rh_2)$ for $Rh_2b_4^{2+}$ corresponds to a diatomic force constant of 0.22 mdyn/Å. All of the available comparisons indicate that the $^3A_{2u}$ ($d\sigma^* \rightarrow p\sigma$) state is more than halfway toward a full Rh–Rh single bond (60–75%). However, the single-bond reference complex has a metal–metal bond that is likely to be somewhat weakened by the chloride axial ligands,[19] which compete for $d\sigma$-bonding, while the $d\sigma^* \rightarrow p\sigma$ excited states of $Rh_2b_4^{2+}$ probed by absorption spectra have little or no axial ligation. Thus, the results appear to be consistent with a $d\sigma^* \rightarrow p\sigma$ Rh_2 excited-state bond order of about $^1/_2$.

The band tentatively assigned to a triplet $d\sigma^* \rightarrow p\sigma^*$ transition at $\sim$530 nm shows that $\nu(Rh_2)$ in the excited state is $\sim$130 cm^{-1}. The band is too poorly resolved from surrounding stronger absorptions to allow conclusive Franck–Condon simulations.[20,21] However, we can still obtain an estimate of the excited-state Rh–Rh distance (3.01 Å) from Woodruff's correlation.[17] This estimate also corresponds to a Rh–Rh bond order of about $^1/_2$.

The only other vibronic structure resolved in our spectra is in 60 cm^{-1} quanta (triplet $d\sigma^* \rightarrow p\sigma$) and in $\nu(C{\equiv}N)$ (several transitions). We believe that the small distortions along the normal coordinate of the 60-cm^{-1} mode indicate that the bridging diisocyanide ligand must make some adjustment, owing to the change in rhodium–rhodium distance. The $\nu(C{\equiv}N)$ vibronic structure is mostly distinguished by the very small values of $S = I(1,0)/I(0,0)$ that are observed (<0.1). Franck–Condon calculations of the distortions in individual C≡N bonds give results <0.01 Å. Thus, the MLCT character of these excited states probably is extremely small.[22] Excited-state $\nu(C{\equiv}N)$ values ($\sim$2150 cm^{-1}) that are very near the ground-state frequencies also indicate little $\pi^*(C{\equiv}N)$ character in the excited state.

Rhodium–Rhodium Bond Strengths. Estimates of Rh_2 bond strengths (D_0 values) are based on the relationship[6,21]

$$D_0(^3A_{2u}) - D_0(^1A_{1g}) = E_0(^3A_{2u}, \text{monomer}) - E_0(^3A_{2u}, \text{dimer}) = \Delta E$$

If we assume that the spectroscopic 0–0 energies (E_0 values) are those of $Rh_2b_4^{2+}$ (38 kcal/mol) and $Rh(CNCMe_3)_4^+$ (62 kcal/mol),[23] then ΔE = 24 kcal/mol.

(16) In the simulated spectrum shown in Figure 7, the 60-cm^{-1} split doublets are generated by assuming two electronic origins, the higher energy one having 70% as much intensity as the lower. We also have performed calculations assuming the 60 cm^{-1} interval to be a symmetric progressional mode; the agreement with experiment was slightly improved in that the valleys between the doublets were filled by an (unresolved in the calculated spectrum) $n(149\ cm^{-1}) + 2(60\ cm^{-1})$ progression, but the best-fit ΔQ was not changed. The ΔQ value is insensitive to the method employed in the generation of the 60-cm^{-1} feature because combinations involving two or more 60-cm^{-1} quanta are weak. The calculated emission spectrum, incidentally, showed little vibronic structure; the 85- and 60-cm^{-1} progressional modes convolute with the 70-cm^{-1} line width to wash out individual vibronic features.

(17) Woodruff's relationship is an empirical correlation of force constants and bond distances: Miskowski, V. M.; Dallinger, R. F.; Christoph, G. G.; Morris, D. E.; Spies, G. H.; Woodruff, W. H. *Inorg. Chem.* **1987**, *26*, 2127–2132. The equation for 4d–4d complexes is r (Å) = 1.83 + 1.45[exp(−F/2.53)], where F is the force constant in mdyn/Å: Woodruff, W. H., unpublished results.

(18) Miskowski, V. M.; Smith, T. P.; Loehr, T. M.; Gray, H. B. *J. Am. Chem. Soc.* **1985**, *107*, 7925–7934.

(19) Miskowski, V. M.; Gray, H. B. In *Understanding Molecular Properties*; Avery, J.; Dahl, J. P., Eds.; Reidel Publishing Co.: Dordrecht, Holland, 1987.

(20) Nonetheless, Franck–Condon calculations[21] that tried to simulate the intensity variation of the observed vibronic features near the maximum yielded a reasonable excited-state Rh–Rh distance, 3.02 Å.

(21) Rice, S. F. Ph.D. Thesis, California Institute of Technology, 1982.

(22) Resonance Raman studies confirm this interpretation, as only exceedingly weak $\nu(C{\equiv}N)$ could be observed upon resonance (514.5 nm) excitation of $Rh_2b_4^{2+}$ $^1A_{1g} \rightarrow {}^1A_{2u}$ ($d\sigma^* \rightarrow p\sigma$) in CH_3CN or DMF solution. A good example of an authentic MLCT transition involving $\pi^*(C{\equiv}N)$ is a band of $Cr(NH_3)_5CN^{2+}$ at 220 nm, which shows a long progression in an excited-state $\nu(C{\equiv}N)$ of 1600 cm^{-1}: Riccieri, P.; Zinato, E. *Inorg. Chem.* **1980**, *19*, 853–859.

(23) Spectra of $Rh(CNCMe_3)_4^+$ were measured in PMMA films at 15 K. Our assignments agree with the literature (Isci, H.; Mason, W. R. *Inorg. Chem.* **1975**, *14*, 913–918). Since the vibronic structure of the $^1A_{1g} \rightarrow {}^3A_{2u}$ ($d_{z^2} \rightarrow p_z$) transition was not resolved, a standard approximation (Fleischauer, P. D.; Adamson, A. W.; Sartori, G. In *Inorganic Reaction Mechanisms, Part II*; Edwards, J. O., Ed.; Wiley: New York, 1972) was used to estimate the energy of the 0–0 transition.

We have taken two approaches in attempts to obtain the D_0 values. First, we have estimated the excited-state bond energy by a Birge–Sponer extrapolation[24] of the observed vibronic levels. In this extrapolation, a plot of the energy of a given vibrational level ($G_0(v)$) minus E_0 divided by the number of vibrational quanta (v) should yield a straight line. The dissociation energy (D_0) is then given by the square of the intercept divided by 4 times the slope.

The experimental plot is not a straight line (Figure 8). However, Birge–Sponer plots usually show negative curvature as the dissociation limit is approached, because higher terms in the vibrational energy expansion become important.[24] The positive curvature observed for $Rh_2b_4^{2+}$ at high v is probably due to the ligands; as the outer turning-point distortion at high v becomes large, the bridging groups must necessarily start to contribute to the restoring force for the vibration. We have estimated a D_0 of 42 kcal/mol from the slope derived from the vibrational levels with $v < 15$. The excited-state D_0 yields a ground-state bond energy of 18 kcal/mol.

A second estimate has been obtained from the temperature dependence of K_{eq} for the dimerization of $Rh(CNPh)_4^+$ in acetonitrile solution, resulting in the parameters $\Delta S = -15$ eu and $\Delta H = -6.3$ kcal/mol.[21] On the basis of 6 kcal/mol as the dimer ground-state D_0, the excited-state bond energy is calculated to be 30 kcal/mol. However, the value of 6 kcal/mol is likely to be an underestimate, because it neglects the differential solvation of the monomer and dimer.

If we assume that the two estimation methods define upper and lower limits, then the excited-state and ground-state Rh–Rh bond energy ranges are 36 ± 6 and 12 ± 6 kcal/mol. The values 36 and 12 kcal/mol are consistent with a well-established rule that force constants for closely related diatomic molecules are proportional to bond energies,[25] because the ratio of diatomic force constants for the $^3A_{2u}$ and $^1A_{1g}$ states is 3:1.

Acknowledgment. We thank Terry Smith for assistance with the Raman experiments. S.F.R. acknowledges a Fannie and John Hertz Fellowship. This research was supported by National Science Foundation Grant CHE84-19828.

(24) Birge, R. T.; Sponer, H. *Phys. Rev.* **1926**, *28*, 259–283.

(25) Nakamoto, K. *Infrared Spectra of Inorganic and Coordination Compounds*, 2nd ed.; Wiley-Interscience: New York, 1970; p 9.

Contribution No. 7691 from the Arthur Amos Noyes Laboratory, California Institute of Technology, Pasadena, California 91125

Vibrational and Electronic Spectra of $Ru_2(O_2CH)_4^+$

Vincent M. Miskowski,*[1a] Thomas M. Loehr,*[1b] and Harry B. Gray*[1a]

Received December 15, 1987

Vibrational (near-infrared and Raman) spectra of $Ru_2(O_2CH)_4Cl$ and $K[Ru_2(O_2CH)_4Cl_2]$ indicate values of $\nu(Ru_2) \simeq 330$ cm^{-1}, symmetric and asymmetric ν(RuCl) of 200 and 150 cm^{-1}, and ν(RuO) of ~430 (a_{1g}) and ~470 cm^{-1} (e_u). Near-infrared low-temperature electronic spectra place the $\delta \rightarrow \delta^*$ and $\pi^* \rightarrow \delta^*$ electronic transitions at ~9000 and ~7000 cm^{-1}, respectively. For both chloro complexes, and also for $[Ru_2(O_2CH)_4Br_2]^-$ (formed in KBr), three vibrations coupled to $\delta \rightarrow \delta^*$ have similar Franck–Condon factors; excited-state values are $\nu(Ru_2) \approx 275$–310 cm^{-1}, ν(RuO) ≈ 420–440 cm^{-1}, and $\nu \approx 140$–210 cm^{-1} attributable to $\delta(Ru_2O)$ or ν(Ru–halide). The vibronic intensities observed for the formate complexes are compared to those of other carboxylate derivatives, and it is concluded that strong vibrational coupling of $\nu(Ru_2)$ with other vibrational modes is present in the formates.

We recently reported[2] a comprehensive spectroscopic study of $Ru_2(O_2CR)_4X$ and $[Ru_2(O_2CR)_4X_2]^-$ (X = Cl, Br; R = methyl, ethyl, *n*-propyl). We were able to locate several metal–metal excited states of these $^4(\pi^{*2}\delta^{*1})$ ground-state compounds, including $\delta \rightarrow \delta^*$ at ~9000 cm^{-1} and the very weak spin-forbidden $\pi^* \rightarrow \delta^*$ at ~7000 cm^{-1}.

Since the available theoretical calculation[3] is for a formate complex, $[Ru_2(O_2CH)_4Cl_2]^-$, it seemed important to establish that the Ru_2(II,III) formates had electronic spectra similar to those of the other carboxylates. Photoelectron spectra[4] show that the metal–metal ionization energies of $Mo_2(O_2CH)_4$ are blue-shifted by about 1 eV from those of $Mo_2(O_2CCH_3)_4$, although their electronic transition energies are virtually the same.[5] It turns out that the transition energies also are very similar in all the Ru_2(II,III) carboxylate complexes, but the vibronic structure associated with $\delta \rightarrow \delta^*$ in the formate differs from that of the other carboxylates.

Table I. Vibrational Spectral Data (cm^{-1}) for Solid $Ru_2(O_2CH)_4Cl$ and $K[Ru_2(O_2CH)_4Cl_2]$

	$Ru_2(O_2CH)_4Cl$ (I)	$K[Ru_2(O_2CH)_4Cl_2]$ (II)
	Raman	
$\delta(Ru_2O)$	135 m	124 vw
ν_s(RuCl)	157 m	150 s
a_{1g} δ_s(RuO)	194 m	193 s
δ(RuO)	281 vw	276 vw
a_{1g} $\nu(Ru_2)$	331 vs	335 s
a_{1g} ν(RuO)	440 m	426 s
ν(RuO)	465 vw	464 vw
	IR	
δ(RuO) or δ(RuCl)		150 m
ν(RuCl)	212 s	200 s
$\nu(RuO_2)$	262 s	278 s
ν(RuO)	406 vw	405 w
	465 vs	419 w
	464 vs	464 vs
	496 s	495 s

Experimental Section

Preparations of $Ru_2(O_2CH)_4Cl$[6] and $K[Ru_2(O_2CH)_4Cl_2]$[7] followed literature procedures. Equipment and procedures used in this study were

(1) (a) California Institute of Technology. (b) Oregon Graduate Center.
(2) Miskowski, V. M.; Loehr, T. M.; Gray, H. B. *Inorg. Chem.* **1987**, *26*, 1098.
(3) Norman, J. G., Jr.; Renzoni, G. E.; Case, D. A. *J. Am. Chem. Soc.* **1979**, *101*, 5256.
(4) Cotton, F. A.; Norman, J. G., Jr.; Stults, B. R.; Webb, T. J. *J. Coord. Chem.* **1976**, *5*, 217.
(5) Norman, J. G., Jr.; Kolari, H. J.; Gray, H. B.; Trogler, W. C. *Inorg. Chem.* **1977**, *16*, 987.
(6) Mukaida, M.; Nomura, T.; Ishimori, T. *Bull. Chem. Soc. Jpn.* **1972**, *45*, 2143.
(7) Bino, A.; Cotton, F. A.; Felthouse, T. R. *Inorg. Chem.* **1979**, *18*, 259.

0020-1669/88/1327-4708$01.50/0